



THE UNIVERSITY *of* EDINBURGH

Edinburgh Research Explorer

Characterization of photomorphogenic responses and signaling cascades controlled by phytochrome-A expressed in different tissues

Citation for published version:

Kirchenbauer, D, Viczián, A, Ádám, É, Hegeds, Z, Klose, C, Leppert, M, Hiltbrunner, A, Kircher, S, Schäfer, E & Nagy, F 2016, 'Characterization of photomorphogenic responses and signaling cascades controlled by phytochrome-A expressed in different tissues: Photomorphogenesis in far-red light', *New Phytologist*.
<https://doi.org/10.1111/nph.13941>

Digital Object Identifier (DOI):

[10.1111/nph.13941](https://doi.org/10.1111/nph.13941)

Link:

[Link to publication record in Edinburgh Research Explorer](#)

Document Version:

Peer reviewed version

Published In:

New Phytologist

General rights

Copyright for the publications made accessible via the Edinburgh Research Explorer is retained by the author(s) and / or other copyright owners and it is a condition of accessing these publications that users recognise and abide by the legal requirements associated with these rights.

Take down policy

The University of Edinburgh has made every reasonable effort to ensure that Edinburgh Research Explorer content complies with UK legislation. If you believe that the public display of this file breaches copyright please contact openaccess@ed.ac.uk providing details, and we will remove access to the work immediately and investigate your claim.



**Characterization of photomorphogenic responses and signaling cascades
controlled by phytochrome-A expressed in different tissues**

Daniel Kirchenbauer^{1*}, András Viczián^{2*}, Éva Ádám², Zoltán Hegedűs³, Cornelia
Klose¹, Michael Leppert¹, Andreas Hiltbrunner^{1,4}, Stefan Kircher¹, Eberhard
Schäfer^{1,4}, Ferenc Nagy^{2,5}

¹Faculty of Biology, Institute of Molecular Plant Physiology, University of Freiburg,
Schänzlestrasse 1, D-79104 Freiburg, Germany.

²Institute of Plant Biology, Biological Research Centre, Temesvári krt.62, H-6726
Szeged, Hungary.

³Institute of Biophysics, Biological Research Centre, Temesvári krt.62, H-6726
Szeged, Hungary.

⁴BIOSS Centre for Biological Signalling Studies, University of Freiburg, 79104
Freiburg, Germany

⁵Institute of Molecular Plant Science, School of Biological Sciences, University of
Edinburgh, Edinburgh EH9 3JH, UK

Corresponding author:

Ferenc Nagy

Phone: 00-36-62599718

Fax: 00-36-62433434

E-mail: nagy.ferenc@brc.mta.hu

* These authors contributed equally to this work.

Running title:

Photomorphogenesis in far-red light

Key words:

Arabidopsis thaliana, signaling, tissue/cell specificity, transcription,
photomorphogenesis, phytochrome A

Word count:

Introduction: 1140

35 Materials and Methods: 643

36 Results: 2747

37 Discussion: 1857

38 Acknowledgement: 96

39 Total: 6483

40

41

42 Number of figures: 7

43 Figures in color: Fig. 1, Fig. 5, Fig. 7

44

45 Supporting Information

SUMMARY

(1) The photoreceptor phytochrome A acts as a light-dependent molecular switch and regulates responses initiated by very low fluences of light (VLFR) and high fluences (HIR) of far-red light. PhyA is expressed ubiquitously, but how phyA signaling is orchestrated to regulate photomorphogenesis is poorly understood.

(2) To address this issue, we generated transgenic *Arabidopsis thaliana* *phyA-201* mutant lines expressing the biologically active PHYA-YFP photoreceptor in different tissues, and analyzed the expression of several reporter genes, including HY5-GFP and CFP-PIF1 and various FR-HIR dependent physiological responses.

(3) We show that phyA action in one tissue is (i) critical and sufficient to regulate flowering time, and root growth; (ii) control of cotyledon and hypocotyl growth requires simultaneous phyA activity in different tissues, and (iii) changes detected in the expression of reporters are not restricted to phyA-containing cells.

(4) We conclude that FR-HIR-controlled morphogenesis in *Arabidopsis* is mediated partly by tissue-specific and partly by intercellular signaling initiated by phyA. Intercellular signaling is critical for many FR-HIR induced responses, yet it appears that phyA modulates the abundance and activity of key regulatory transcription factors in a tissue-autonomous fashion.

INTRODUCTION

Plants are sessile organisms, and to optimize their fitness and competitiveness they must adapt to changes in their abiotic and biotic environment. From among the numerous environmental factors light is arguably the most important one, since plants use light not only as the energy source for photosynthesis but also as a developmental cue. To harmonize their growth and development with the ambient light environment, plants have evolved a battery of highly specialized photoreceptors. These photoreceptors monitor the quality, quantity, duration and direction of the incident sunlight and include the UVB-sensing UVB-RESISTANCE 8 (Rizzini *et al.*, 2011), the blue/UVA light absorbing cryptochromes, phototropins and ZTL-like photoreceptors (Christie, 2007; Yu *et al.*, 2010; Chaves *et al.*, 2011) and the red (R) and far-red (FR) light absorbing phytochromes (Franklin & Quail, 2010). Phytochromes (phy) are chromoproteins that exist as dimers, and each monomer contains a covalently linked open tetra-pyrrol chain chromophore. In the model plant *Arabidopsis thaliana* the phytochromes are encoded by a small multigene family (Sharrock & Quail, 1989; Clack *et al.*, 1994). Phytochromes cycle between their biologically inactive (Pr) and active (Pfr) forms and act as light quality/quantity dependent molecular switches. phyA is a highly specialized far-red sensor, since a very low level of phyA Pfr (~0.1 % of total phyA) generated by FR or a low-ratio R/FR light is already sufficient to launch signaling. It follows that phyA regulates the so-called very low fluence (VLFR) and high-irradiation responses to far-red light (FR-HIR), and thereby plays a dominant role in mediating transition from skotomorphogenesis to photomorphogenesis (Casal *et al.*, 2014).

According to the generally accepted concept, the overwhelming majority of molecular events underlying phyA-controlled photomorphogenesis take place in the nucleus. Light in a quality- and quantity-dependent fashion induces translocation into and accumulation of phyA Pfr in the nuclei (Kircher *et al.*, 1999). PhyA does not have endogenous nuclear localization signal (NLS) motifs, and import of phyA Pfr is mediated by the NLS-containing FAR-RED ELONGATED HYPOCOTYL1 and FHY1-like proteins that shuttle between the nucleus and the cytoplasm (Hiltbrunner *et al.*, 2005; Hiltbrunner *et al.*, 2006; Rausenberger *et al.*, 2011). PhyA Pfr localized in the nucleus interacts with a battery of negative regulatory proteins, including CONSTITUTIVE PHOTOMORPHOGENIC1 (COP1), SUPPRESSOR OF PHYA-105 1-4 (SPA1-4) and PHYTOCHROME INTERACTING FACTORS (PIFs). The

104 very early steps of phyA signaling result in (i) the inactivation or alteration of the
 105 substrate specificity of the COP1/SPA1-4 complex that targets proteins to
 106 degradation, (ii) disruption of the binding of PIF transcription factors (TFs) to their
 107 cognate promoters and/or initiating their degradation, and (iii) induction of
 108 transcriptional cascades that modulate the expression of 2500–3000 genes of the
 109 Arabidopsis genome in a FR light-dependent fashion (Tepperman *et al.*, 2001). In this
 110 aspect it is worth noting that phyA is ubiquitously expressed (Somers & Quail, 1995;
 111 Hall *et al.*, 2001), and FR light readily penetrates plant tissues. It follows that phyA
 112 signaling, at least theoretically, can be induced simultaneously in each cell. If so, then
 113 it would be essential to know to what extent phyA signaling in different cells/tissues
 114 is identical and/or different, and how these signaling cascades are interconnected with
 115 each other to regulate complex photomorphogenic responses such as hypocotyl
 116 growth inhibition or cotyledon expansion. Clearly, a prerequisite to answer these
 117 questions is to collect detailed information about the spatial/temporal features of
 118 phyA-controlled signaling cascades. The first reports addressing this problem
 119 produced data obtained by focused irradiation (spot, micro-beam etc.) targeted to
 120 specific parts/organs/tissues. For example, it was shown that phytochrome localized in
 121 leaves is essential for regulating hypocotyl elongation under shade conditions (Casal
 122 & Smith, 1988a; Casal & Smith, 1988b). Nick *et al.* (1993) reported that
 123 accumulation of anthocyanin and *CHALCONE SYNTHASE* mRNA induced by
 124 microbeam irradiation with FR light in the cotyledons of mustard seedlings is a cell-
 125 autonomous, stochastic response. However, to explain the gradually developing
 126 expression pattern at the whole organ level these authors hypothesized that the
 127 responses of individual cells are integrated by inhibitory, intercellular communication.
 128 Bischoff *et al.* (1997) showed that microbeam irradiation with R light induced
 129 expression of the *CAB:LUC* reporter at distant parts of the transgenic tobacco leaves,
 130 a finding that indicates existence of inductive cell-to-cell signaling. Jordan *et al.*
 131 (1995) concluded that manipulation of spatial distribution by over-expressing oat
 132 phyA in different organs in transgenic tobacco results in different phenotypes, and
 133 that phyA localized in the vascular tissue plays a significant role in regulating stem
 134 elongation by repressing gibberellic acid (GA) biosynthesis. Neuhaus *et al.* (1993)),
 135 Bowler *et al.* (1994) and Kunkel *et al.* (1996) used a radically different approach,
 136 namely microinjection of phyA and various other putative signaling compounds into
 137 the tomato *aurea* mutant, which is deficient in photoactive phytochromes. These

138 authors demonstrated that phyA signals in a cell-autonomous fashion in a subset of
139 hypocotyl cells, but these studies lacked analysis of complex developmental responses
140 and were limited in time. More recently, Warnasooriya and Montgomery (2009) and
141 Costigan *et al.* (2011) chose a different approach and analyzed FR-HIR induced
142 responses in transgenic Arabidopsis plants in which accumulation of the chromophore
143 required for the activity of all phytochromes was decreased in an organ/tissue specific
144 fashion by expressing plastid-targeted mammalian biliverdin IX alpha reductase under
145 the control of selected promoters. These authors concluded that phyA-controlled
146 developmental responses, including hypocotyl growth inhibition and root elongation
147 are mediated by long-distance, inter-organ signaling. The caveat of this approach is
148 that it lowers rather than fully inhibits accumulation of the chromophore, and the
149 precise amount of the active photoreceptor present in the various tissues/organs is not
150 known.

151 Whilst these studies revealed important spatial/temporal features of phyA-controlled
152 photomorphogenic responses, they provided limited molecular information about the
153 events of phyA-controlled signaling cascades at the molecular level. phyA contains no
154 DNA-binding motifs, but Chen *et al.* (2014) demonstrated by chromatin
155 immunoprecipitation sequencing and RNA sequencing methods that phyA associates
156 with the promoters of hundreds of not only FR light induced but also stress/hormone
157 regulated genes. These authors postulated that by relying on this mechanism phyA has
158 the capacity to directly regulate rapid adaptation of plants to their changing
159 environment by controlling/integrating multiple biological processes. However, these
160 experiments were not designed to address whether phyA binding to the promoters is
161 different in different cell types, thus provided little if any information about the spatial
162 aspects of phyA signaling.

163 To obtain more precise information about the tissue specificity of molecular events
164 mediating phyA signaling in FR-HIR, we chose a yet different approach. Namely, we
165 (i) generated transgenic lines expressing the phyA-YFP (YELLOW FLUORESCENT
166 PROTEIN) fusion protein in the *phyA-201* mutant under the control of its own as well
167 as different tissue-specific promoters, (ii) characterized a broad array of FR-HIR
168 light-induced developmental responses at the physiological level, and (iii)
169 complemented these studies by analyzing the accumulation/degradation of specific
170 reporter constructs in the wild type and/or in transgenic lines expressing the phyA-
171 YFP photoreceptor in different tissues.

172 MATERIALS AND METHODS

173

174 Cloning, generation of transgenic plants

175 For details of constructing the transgenes used in this study, see Supporting
176 Information Methods S1 and Supporting Information Table S1. Throughout the study
177 we used *Arabidopsis thaliana* L. (Heynh.) *phyA-201* mutant (Reed *et al.*, 1993), (Ler
178 ecotype). The chimeric constructs were transformed into *Arabidopsis* as described by
179 Clough & Bent, (1998). Independent homozygous lines expressing one Mendelian
180 copy of the transgene were selected for further analysis.

181

182 Seedling and plant growth conditions

183 Surface sterilized seeds stratified for 72 h in the dark (4 °C), after which germination
184 was induced by 18 h of white light (20 $\mu\text{mol m}^{-2} \text{s}^{-1}$, 22 °C). The plates were
185 subsequently treated as specified in the text. For analysis of flowering time, seeds
186 were sown on soil, stratified for 72 h in the dark (4 °C) and subsequently treated as
187 specified.

188

189 Microscopy techniques

190 Epifluorescent and light microscopy was performed as described by Bauer *et al.* (
191 2004). Confocal laser scanning microscopy was performed using a Leica SP5 AOBS
192 confocal laser scanning microscope (Leica, Germany) on DMI6000 microscope base.
193 Microscope configuration was the following: objective lens: HC PL APO 20x
194 (NA:0.7); sampling speed: 100 Hz; line averaging: 3x; pinhole: 200 μm ; scanning
195 mode: sequential unidirectional; excitation: 488 nm laser (GREEN FLUORESCENT
196 PROTEIN, GFP), 514 nm laser (YFP); spectral emission detectors: 496-518 nm
197 (GFP), 545-582 nm (YFP). Brightness and contrast settings were uniformly done on
198 the corresponding image pairs. GFP and YFP images were pseudo-colored green and
199 red, respectively. All microscopic manipulations were performed under safe green
200 light and documentation of cells was performed during the first 60 s of microscopic
201 analysis. In each experiment at least 20 seedlings from 4 independent transgenic lines
202 (representing >100 cells/seedling) were analyzed and statistically evaluated.
203 Frequencies of images supporting or contrasting the conclusions drawn was >95% or
204 0.1%. Every experiment was repeated 3 times.

205

206 **Hypocotyl length and cotyledon area measurement**

207 After induction of germination, seeds were placed at 22 °C in darkness or in FR light
208 ($20 \mu\text{mol m}^{-2} \text{s}^{-1}$, 730 nm, 128 nm full widths at half-maximum). Measurement of
209 hypocotyl length and cotyledon area was performed as described by *Ádám et al.*
210 (2013). At least 25 seedlings were used for each line and each experiment.

211

212 **Analysis of flowering time**

213 Following stratification, seedlings were grown in short day (8 h white light; $130 \mu\text{mol}$
214 $\text{m}^{-2} \text{s}^{-1}$ /16 h dark) or in short day extended by 8 h FR light (8 h white light; $130 \mu\text{mol}$
215 $\text{m}^{-2} \text{s}^{-1}$ /8 h far red light; $30 \mu\text{mol m}^{-2} \text{s}^{-1}$ / 8 h dark). Irradiation with FR light was
216 performed in a FR light field (730 nm, 128 nm full width at half-maximum). After 15
217 days, all plants were grown in short day without FR irradiation. Flowering time of
218 each plant was determined by counting the days until flower buds became visible in
219 the centre of the rosette. At least 9 plants were used for each line and light condition.
220 All experiments were repeated two times.

221

222 **Analysis of phototropism**

223 Seeds were sown on rectangular $\frac{1}{2}$ MS (Murashige and Skoog medium) agar plates
224 covered with one sheet of sterilized filter paper. After stratification, the plates were
225 incubated vertically for 2 days in darkness (23°C). The seedlings were irradiated with
226 far-red light ($10 \mu\text{mol m}^{-2} \text{s}^{-1}$) for 120 min. Unilateral blue light irradiation ($1 \mu\text{mol m}^{-2}$
227 s^{-1}) was supplied for 160 min by a projector (Leitz, Wetzlar, Germany) equipped
228 with a blue light filter (KG45; Optic Balzers, Liechtenstein). For homogeneous
229 illumination of the etiolated seedlings the plates were placed with an angle of 3° to the
230 light axis. After scanning of the plates hypocotyl bending was measured with ImageJ
231 (Schneider *et al.*, 2012).

232

233 **Root growth measurements**

234 Seeds were sown on rectangular $\frac{1}{2}$ MS agar plates containing 1% of sucrose. The
235 plates were incubated vertically for 10 days in far-red light ($20 \mu\text{mol m}^{-2} \text{s}^{-1}$) at 22 °C.
236 The plates were scanned and root length was measured with ImageJ.

237

238

239 **RESULTS**

240 **Generation of transgenic *phyA-201* lines expressing phyA-YFP in tissue-specific**
241 **fashion**

242 To ensure tissue/cell type specific localization of the functional phyA-YFP
243 photoreceptor *in planta*, we expressed the fusion protein under the control of *PHYA*,
244 *MERISTEM LAYER 1* (*ProML1*), *SUCROSE (SUC)/H⁺ SYMPORTER 2* (*ProSUC2*)
245 and *CHLOROPHYLL A/B BINDING PROTEIN 3* (*ProCAB3*) promoters in the *phyA-*
246 *201* mutant. The *ProPHYA* promoter is known to be ubiquitously expressed in
247 seedlings (Somers & Quail, 1995; Hall *et al.*, 2001), whereas the *ProCAB3*, *ProML1*
248 and *ProSUC2* promoters had been routinely used in the past to express proteins of
249 interest exclusively in mesophyll, epidermal or companion cells, respectively
250 (Sessions *et al.*, 1999; Srivastava *et al.*, 2008; Hategan *et al.*, 2014). For this study we
251 raised 15–20 independent transgenic lines for each construct, and selected those
252 which segregated the transgenes as a single Mendelian trait. Transgenic lines
253 homozygous for the *ProML1:PHYA-YFP*, *ProSUC2:PHYA-YFP* and
254 *ProCAB3:PHYA-YFP* transgenes were then further characterized by western blot,
255 epifluorescence and confocal microscopy to determine the abundance and tissue-
256 specificity of the respective fusion protein. We selected 4 transgenic lines for each
257 construct, and performed all experiments by using progenies of these lines. We also
258 crossed the selected *ProML1:PHYA-YFP*, *ProSUC2:PHYA-YFP* and
259 *ProCAB3:PHYA-YFP* plants and produced lines expressing the phyA-YFP in two or
260 three tissue types. For a detailed description of the method applied to identify these
261 multiple transgenic lines see Supporting Information Methods S1 and Fig. S1. The
262 transgenic lines were then used to extend and to corroborate results obtained by the
263 analysis of the parental lines. Fig. 1 shows the typical cellular distribution patterns of
264 the phyA-YFP protein in the cotyledons and in the hook region of the hypocotyls of
265 chosen *ProPHYA:PHYA-YFP*, *ProML1:PHYA-YFP*, *ProSUC2:PHYA-YFP*,
266 *ProCAB3:PHYA-YFP* transgenic lines, and demonstrates that, depending on the
267 promoter used, the phyA-YFP fusion protein is detectable either in each cell type
268 (*ProPHYA*, g-l) or only in the epidermal (*ProML1*, m-r), companion (*ProSUC2*, s-x)
269 or mesophyll (*ProCAB3*, y-ad) cells. Western blot analysis showed that the total
270 amount of phyA-YFP in the *ProPHYA:PHYA-YFP* lines is comparable to that of
271 native phyA in wild type (WT) seedlings (Fig. S2a), but it is approximately 10-12
272 times lower in the *ProML1:PHYA-YFP*, *ProSUC2:PHYA-YFP* and *ProCAB3:PHYA-*
273 *YFP* transgenic lines (Fig. S2b). To compare the abundance of the phyA-YFP fusion

274 protein in different tissues we determined the amount of phyA-YFP accumulated in
 275 nuclei of epidermal and sub-epidermal cells of hypocotyls after 24 h irradiation with
 276 FR light. We found that abundance of the phyA-YFP fusion protein in the epidermal
 277 cells of *ProML1:PHYA-YFP* and *ProPHYA:PHYA-YFP* does not differ significantly,
 278 but it is much (4-5-fold) lower in the sub-epidermal cells of *ProCAB3:PHYA-YFP* as
 279 compared to *ProPHYA:PHYA-YFP* (Fig. S3). Quantitation of phyA abundance in the
 280 companion cells of the various lines was not feasible by this method; however,
 281 microscopic analysis indicates that the expression level of fusion protein is similar in
 282 the selected *ProSUC2:PHYA-YFP* and *ProPHYA:PHYA-YFP* lines (Fig. 1 l, x).
 283 Finally, we compared the expression patterns of the photoreceptor in
 284 *ProPHYA:PHYA-YFP* and the triple transgenic line (obtained by consecutive
 285 crossings of the single *ProML1:PHYA-YFP* with *ProCAB3:PHYA-YFP* and
 286 *ProSUC2:PHYA-YFP*; *ProML1+ProCAB3+ProSUC2:PHYA-YFP*) by confocal
 287 microscopy. Table S2 summarizes the results of these experiments and Fig. S4-S10
 288 illustrate that phyA-YFP is detectable in the epidermis, subepidermal and companion
 289 cells of cotyledons, hypocotyls and various tissues of the root of *ProPHYA:PHYA-*
 290 *YFP* seedlings. Expression of phyA-YFP in the
 291 *ProML1+ProCAB3+ProSUC2:PHYA-YFP* ,triple transgenic line is detectable in the
 292 epidermis, mesophyll and companion cells of cotyledons (Fig. S4,S5), in the
 293 epidermis in the hook and both in the lower and upper part of hypocotyls (Fig. S6-S8)
 294 but its expression in the subepidermal cells of hypocotyls is restricted to the hook
 295 region (Fig. 1l,x) whereas in the root we could only detect phyA-GFP in specific cell
 296 files in the epidermis (located in the division/elongation zone) (Fig. S9,S10). Taken
 297 together, we conclude that the expression pattern and the level of phyA-YFP in the
 298 *ProML1+ProCAB3+ProSUC2:PHYA-YFP* transgenic line mimic *ProPHYA:PHYA-*
 299 *YFP* (i) in the epidermis of cotyledon and hypocotyls and partially in root, (ii)
 300 comparable to that in the companion cells but lower in the subepidermal (mesophyll)
 301 cells of cotyledons and hook region and strongly different (iii) in the subepidermal
 302 cells (cortex) of the upper and lower part of hypocotyls and in the roots.
 303
 304 **Epidermally-expressed phyA-YFP fully restores FR-HIR controlled root growth,**
 305 **but only partially complements the hypocotyl growth inhibition and cotyledon**
 306 **expansion phenotype of the *phyA-201* mutant.**

307 To assess the action of tissue-specifically expressed phyA-YFP we analyzed basic
 308 FR-induced photomorphogenic responses, including promotion of root growth and
 309 cotyledon expansion as well as inhibition of hypocotyl elongation in the selected
 310 transgenic lines. Fig. 2a and Fig. S11a demonstrate that *ProPHYA:PHYA-YFP*,
 311 *ProML1:PHYA-YFP* as well as the *ProML1+ProCAB3+ProSUC2:PHYA-YFP*
 312 transgenic lines exhibited an identical, fully complemented root phenotype. These
 313 figures also show that, in contrast to *ProML1:PHYA-YFP*, the root length of the
 314 *ProCAB3:PHYA-YFP* and *ProSUC2:PHYA-YFP* transgenic seedlings was not
 315 restored. These results suggest that signaling by phyA-YFP localized in the epidermis
 316 is sufficient to fully complement impaired root growth of the *phyA-201* mutant, and
 317 phyA-YFP signaling originated in the mesophyll or companion cells has negligible
 318 effect on controlling this process.
 319 Fig. 2b and Fig. S11b demonstrate that *ProPHYA:PHYA-YFP* in *phyA-201* seedlings
 320 displayed a fully restored, even slightly exaggerated FR-induced cotyledon expansion
 321 phenotype. *ProML1:PHYA-YFP* seedlings exhibited a pronounced whereas
 322 *ProCAB3:PHYA-YFP* seedlings showed a weaker but significant response as
 323 compared to WT. In contrast, phyA in the vascular tissue lines was completely
 324 ineffective in promoting cotyledon expansion of *ProSUC2:PHYA-YFP*. Interestingly,
 325 *ProCAB3+ProSUC2:PHYA-YFP* seedlings displayed a partially whereas
 326 *ProML1+ProCAB3:PHYA-YFP* and the *ProML1+ProCAB3+ProSUC2:PHYA-YFP*
 327 transgenic seedlings produced a slightly over-expressing phenotype for FR-induced
 328 cotyledon expansion. Collectively, these data demonstrate that the simultaneous
 329 action of phyA in epidermal and mesophyll cells is critical and sufficient to promote
 330 FR-dependent cotyledon expansion.
 331 Fig. 2c shows that inhibition of hypocotyl growth is fully restored in the
 332 *ProPHYA:PHYA-YFP* lines and partially in *ProML1:PHYA-YFP* lines as compared to
 333 WT. In contrast, phyA-YFP expressed in companion and mesophyll cells was not able
 334 to induce any detectable response. Fig. 2c and Fig. S11c illustrate that the
 335 *ProML1:PHYA-YFP* and *ProML1+ProCAB3+ProSUC2:PHYA-YFP* transgenic
 336 seedlings displayed similarly enhanced FR-induced hypocotyl growth inhibition when
 337 compared to *phyA-201*, but were still significantly longer when compared to WT or
 338 *ProPHYA:PHYA-YFP*. Taken together, we conclude that the action of phyA-YFP
 339 localized in the epidermis contributes to FR-dependent inhibition of hypocotyl

340 growth, but signaling by phyA localized in different cell/tissue types is also required
341 to fully complement the phenotype of the *phyA-201* mutant.
342 To test if the apparently prominent role of epidermis-localized phyA in regulating FR-
343 dependent hypocotyl and root elongation as well as cotyledon expansion was due to
344 its altered stability, we determined the degradation kinetics of phyA-YFP in
345 *ProML1:PHYA-YFP* and *ProPHYA:PHYA-YFP* transgenic lines by *in vivo*
346 spectroscopy. Fig. S12 demonstrates that degradation of the phyA-YFP fusion protein
347 in *ProML1:PHYA-YFP* is identical to that of the total phyA in *ProPHYA:PHYA-YFP*
348 seedlings. Thus we conclude that degradation of phyA is comparable in different
349 tissues, and tissue-specific differential degradation does not play a major role in
350 regulating phyA signaling.

351

352 **Blue light induced phototropism is modulated by phyA-YFP localized in** 353 **mesophyll cells**

354 In Arabidopsis, blue light dependent phototropism is primarily mediated by the
355 *PHOTOTROPIN* photoreceptors, but blue light induced bending of hypocotyls was
356 shown to be affected by phyA (Janoudi *et al.*, 1997). It was even found that the early
357 phototropic response in blue light is blocked in *phyA* mutant background (Kami *et al.*,
358 2012). The mechanism by which the ubiquitously expressed phyA modulates this
359 early phototropic response is unknown, thus we were interested in determining the
360 spatial requirements for phyA action. To this end we grew transgenic *phyA-201*
361 seedlings expressing the phyA-YFP fusion in tissue-specific fashion in darkness, and
362 illuminated them with unilateral blue light after FR pre-irradiation for 120 min. Fig. 3
363 demonstrates that *ProPHYA:PHYA-YFP* seedlings exhibit a fully complemented
364 response, *ProCAB3:PHYA-YFP* a significant response (50% complementation),
365 whereas phototropic curvatures of *ProML1:PHYA-YFP* and *ProSUC2:PHYA-YFP*
366 seedlings in blue light did not differ from that of the *phyA-201* mutant. To corroborate
367 these data we also determined the phototropic response of *ProML1+ProCAB3:PHYA-*
368 *YFP* and *ProML1+ProCAB3+ProSUC2:PHYA-YFP* transgenic seedlings. We found
369 that phototropic curvature of the double and triple transgenic seedlings was identical
370 to that of *ProCAB3:PHYA-YFP* (Fig. 3). Collectively, these data suggest that for
371 phyA-modulated phototropism (i) signaling by phyA-YFP localized in companion
372 and epidermal cells is largely dismissible, and (ii) the action of phyA-YFP in sub-

epidermal, mainly in the cortical cells of the hook region plays an important role to regulate blue light induced early phototropic response.

phyA-YFP localized in companion cells of vascular bundles regulates FR-accelerated transition to flowering

It has been shown that, similarly to the CRYPTOCHROME2 blue light receptor, *phyA* is involved in regulating the time of flowering in *Arabidopsis* (Mockler *et al.*, 2003). In contrast to *phyB*, these photoreceptors not only up-regulate the transcription of *CONSTANS* (*CO*) (Endo *et al.*, 2013), but also stabilize *CO* in the long-day afternoon. Accordingly, *phyA* mutants compared to WT flowered late in long day conditions (Neff and Chory 1998) but not in short day conditions when the light period was extended with FR irradiation. (Johnson *et al.*, 1994). To test if the localization of *phyA* is critical for regulating flowering time, we performed the standard FR day-extension assay on transgenic plants expressing the *phyA*-YFP photoreceptor in a tissue-specific fashion. Fig. 4a demonstrates that expression of *phyA*-YFP under the control of the *ProPHYA* promoter resulted in full complementation of the delayed flowering phenotype of the *phyA-201* mutant. *phyA*-YFP localized in epidermal and mesophyll cells appears to be inactive concerning the regulation of flowering time, as *ProML1:PHYA-YFP* and *ProCAB3:PHYA-YFP* lines flowered as late as the *phyA-201* mutant. In contrast, *ProSUC2:PHYA-YFP* plants expressing *phyA*-YFP in vascular bundles exhibited, similarly to *ProPHYA:PHYA-YFP*, a fully complemented response. We also determined the accumulation of *FT* mRNA in the various transgenic lines. Our data clearly demonstrate that FR day-extension induces up-regulation of *FT* transcription in the *ProPHYA:PHYA-YFP* and *ProSUC2:PHYA-YFP* but not in the *ProML1:PHYA-YFP* and *ProCAB3:PHYA-YFP* lines (Fig. 4b). Taken together, we conclude that *phyA*-YFP localized in vascular bundles is necessary and sufficient to regulate FR-induced acceleration of flowering time.

phyA-YFP controls FR-HIR dependent accumulation of HY5-GFP and degradation of CFP-PIF1 fusion proteins in tissue-autonomous manner

Two hallmarks of *phyA*-controlled FR-HIR signaling are FR induced transcription and accumulation of the bZIP type transcription factor ELONGATED HYPOCOTYL

5 (HY5) (Osterlund *et al.*, 2000), and induction of the rapid degradation of the majority of bHLH-type PIF transcription factors (Leivar *et al.*, 2012). These events represent very early steps of phyA-controlled signaling, and play an essential role in establishing the complex signaling network (Ma *et al.*, 2001). Our data show that phyA (Fig. S4-S10) and PIF1 (see later Fig. 6) are highly expressed in all tissues tested, whereas expression level of HY5 (Fig. 5) is low (around the threshold of detection) in etiolated seedlings. To test whether FR light dependent modulation of the abundance of these TFs is altered by manipulating the distribution/localization of the photoreceptor we produced WT, *ProML1:PHYA-YFP* and *ProML1+ProSUC2:PHYA-YFP* and *phyA-201* lines that also expressed *ProHY5:HY5-GFP*, and monitored FR-induced changes in the abundance of HY5-GFP by confocal laser scanning microscopy. Fig. 5 clearly demonstrates that (i) the abundance of HY5-GFP is low in all tissues of etiolated seedlings, and that (ii) FR light promotes accumulation of HY5-GFP only in the cells of those tissues which also express the phyA-YFP photoreceptor. Namely, in wild-type seedlings FR treatment uniformly increased the fluorescence in epidermal, mesophyll and vascular cells, whereas the same treatment, for example, induced accumulation of the HY5-GFP fusion protein only in the epidermis of the *ProML1:PHYA-YFP* line and additionally in the companion cells of *ProML1+ProSUC2:PHYA-YFP* transgenic seedlings. In contrast, FR illumination did not induce expression of *ProHY5:HY5-GFP* in transgenic *phyA-201* lines lacking the active photoreceptor (Fig. S13). We used the same experimental approach to monitor FR-induced degradation of PIF1. PIF1 negatively regulates chlorophyll biosynthesis and seed germination in the dark, and light-induced degradation of PIF1 relieves this negative regulation to promote photomorphogenesis (Huq *et al.*, 2004). We expressed CFP-PIF1 in *ProML1:PHYA-YFP*-harboring *phyA-201* seedlings. Fig. 6 shows that the abundance of CFP-PIF1 is high, and the protein is readily detectable in all cell types of etiolated seedlings. This figure also demonstrates that a short exposure to FR light induced rapid degradation of the fusion protein in the epidermal, mesophyll and companion cells of wild-type seedlings, whereas in the *ProML1:PHYA-YFP* seedlings degradation of the fusion protein was detectable only in the epidermal cells. These data strongly suggest that for controlling PIF1 and HY5 abundances phyA acts in a tissue-autonomous fashion, and intercellular communication between the cells of different tissues does not play a major role.

phyA-YFP regulates FR-HIR dependent transcription of genes in tissue-autonomous and non-tissue-autonomous fashion

We also attempted to characterize to what extent regulation of cFR light dependent transcription of genes is affected by expressing phyA in different tissues. To this end first we selected several genes whose transcription was shown to be up- or down-regulated by FR irradiation (Peschke & Kretsch, 2011). Next we constructed reporters containing promoters of the above genes, the CYANO FLUORESCENT PROTEIN (CFP) reporters and SV-40 NLS, and introduced these chimeric constructs into WT, *ProML1:PHYA-YFP* and *ProML1+ProCAB3+ProSUC2:PHYA-YFP* lines. GIBBERELLIN 2-BETA-DIOXYGENASE 1 (GA2ox1) catalyzes the hydroxylation of GA molecules, thus reduces available bioactive GA (Rieu *et al.*, 2008). The enzyme XYLOGLUCAN ENDOTRANSGLUCOSYLASE/HYDROLASE 17 (XTH17) is involved in the hydrolysis of xyloglucans, and takes part in the restructuring of xyloglucan cross-links in the cellulose/xyloglucan cell wall framework (Vissenberg *et al.*, 2005). Members of the indole-3-acetic acid inducible (IAA) gene family, including IAA19 are transcription regulators act as repressors of auxin-induced gene expression and were shown to be involved in regulating various hypocotyl and root growth responses (Liscum & Reed, 2002; Tian *et al.*, 2004; Jing *et al.*, 2013).

Expression of *ProGA2ox1* is below detection level in the hypocotyls and cotyledons of etiolated seedlings and significantly upregulated by FR treatment in the epidermal and sub-epidermal cells of both organs of WT as well as in triple transgenic seedlings. However FR-induced upregulation of *ProGA2ox1:CFP-NLS* was also readily detected not only in the epidermis but also in the sub-epidermal cells of hypocotyls (Fig. 7) and cotyledons of *ProML1:PHYA-YFP* seedlings (Fig. S14). These data demonstrate that upregulation of *GA2ox1* in the sub-epidermis is mediated by mobile signal(s) generated by phyA action in the epidermis cells. The expression pattern of *ProXTH17* differed from that of *ProGA2ox1*. CFP fluorescence was not detectable in the cotyledon, but was quite strong both in the epidermis and sub-epidermis of the hypocotyl of etiolated WT, *ProML1:PHYA-YFP* and triple transgenic seedlings. Irradiation by FR light radically changed these patterns. FR light upregulated transcription of *ProXTH17* only in the sub-epidermal cells of cotyledons of WT, *ProML1:PHYA-YFP* and triple transgenic seedlings (Fig. S14). These data

indicate that expression of *ProXTH17* is restricted to the mesophyll cells in this organ, and that phyA localized only in the epidermal cells is sufficient to enhance expression of *ProXTH17* in the mesophyll cells. In other words, we conclude that FR light modulated transcription of *ProXTH17* is (i) at least partly regulated by intercellular signaling, (ii) mobile signal(s) generated in the epidermis is/are sufficient to induce its expression in mesophyll cells devoid of phyA. In contrast to cotyledons, FR light strongly down-regulates expression of *ProXTH17* both in the epidermis and the sub-epidermis of the hypocotyl of WT, *ProML1:PHYA-YFP* and triple transgenic seedlings (Fig. 7).

Expression of *ProIAA19:CFP-NLS* displayed a unique pattern. This reporter was not detectable in the cotyledons of dark-grown seedlings, but was highly expressed in the epidermis and sub-epidermis of the hypocotyls of WT, *ProML1:PHYA-YFP* and triple transgenic seedlings (Fig. 7). FR irradiation dramatically reduced expression of the reporter in all cell types in WT seedlings, but was completely ineffective to reduce CFP fluorescence detectable in the epidermis and sub-epidermis of *ProML1:PHYA-YFP* and triple transgenic seedlings. We interpret these results to indicate that the repressor of the transcription of *ProIAA19* is not activated/produced either in the *ProML1:PHYA-YFP* or triple transgenic seedlings. We have shown that the amounts of phyA present in the epidermis of *ProML1:PHYA-YFP*, *ProPHYA:PHYA-YFP* and triple transgenic seedlings do not differ significantly, thus we conclude that signaling launched by phyA localized in the epidermis is not sufficient to down-regulate expression of *ProIAA19* in this tissue. It follows that the signal which is produced either in the sub-epidermal or vascular cells (or both) in WT seedlings is absent or below optimal level in the *ProML1:PHYA-YFP* and triple transgenic lines. Collectively, analysis of the expression characteristics of these four reporter constructs at the cellular resolution level convincingly demonstrates that phyA signaling in FR-HIR is mediated partly by intercellular signaling.

DISCUSSION

We produced transgenic *phyA-201* plants expressing the phyA-YFP photoreceptor under the control of its own promoter or selectively in epidermal, mesophyll and companion cells. By crossings we also generated plants that contain phyA in two or three tissue types. The distribution pattern and abundance of phyA-YFP in the

509 *ProML1+ProCAB3+ProSUC2:PHYA-YFP* line was only partially identical to that of
510 phyA-YFP in the *ProPHYA:PHYA-YFP* line due to the low expression level of the
511 *ProCAB3:PHYA-YFP* transgene and the lack of expression of *ProSUC2:PHYA-YFP*
512 in the hypocotyl and root. We note that the reduced level of phyA in the mesophyll
513 cells is likely due to the fact that the basal level activity of the *ProCAB3* promoter,
514 which itself is highly upregulated by phyA signaling, was sufficient only to induce
515 low level accumulation of phyA in etiolated tissue. Upon FR treatment the activity of
516 the *ProCAB3* promoter is enhanced, but accumulation of phyA is simultaneously
517 reduced by the degradation of phyA Pfr, thus we conclude that the steady-state levels
518 of phyA remained below sub-optimal when compared to *ProPHYA:PHYA-YFP*
519 seedlings.

520 phyA mediates VLFRs, which initiate de-etiolation, and HIRs, which complete
521 de-etiolation under sustained activation with FR. phyA signaling in VLFR and FR-
522 HIR conditions displays characteristic differences and is mediated partly by similar,
523 partly by specific molecular components and events (Casal *et al.*, 2014). The
524 physiological responses brought about by a single or hourly repeated light pulses are
525 generally less robust, and monitoring changes in the expression levels of reporters in
526 VLFR condition requires custom-made, special reporters. To this end we will address
527 tissue autonomous/tissue-to-tissue aspects of phyA signaling in VLFR and the
528 possible inter-dependence of the VLFR and HIR modes of actions of phyA signaling
529 in a separate report.

530 Analysis of FR-HIR induced photomorphogenic responses exhibited by the
531 selected transgenic lines clearly demonstrated that the output of phyA-YFP drastically
532 differs in the different tissues. We show that phyA is capable of regulating a subset of
533 FR-HIR dependent responses in tissue-autonomous fashion (i.e. phyA action in one
534 tissue is sufficient to complement the *phyA-201* phenotype), whereas other responses
535 are clearly regulated by simultaneous phyA signaling in different tissues. For example
536 the *ProSUC2:PHYA-YFP* and *ProPHYA:PHYA-YFP* lines, expressing the
537 photoreceptor in their vascular bundles, fully restore the flowering phenotype of the
538 *phyA-201* mutant. These data demonstrate that phyA-dependent stabilization of CO in
539 the vascular cells can occur without phyA signaling in any other tissues, similarly to
540 CRYPTOCHROME2 (Endo *et al.*, 2007) but in contrast to phyB (Endo *et al.*, 2005).
541 However, it is evident that, beyond regulating flowering time, phyA signaling in the
542 companion cells also contributes to FR-induced expansion of cotyledons (compare the

phenotypes of *ProML1:PHYA-YFP*, *ProSUC2:PHYA-YFP* and *ProML1+ProSUC2:PHYA-YFP*, Fig. 2) but appears not to be critical for FR-regulated phototropism and root elongation.

phyA-YFP levels in *ProCAB3:PHYA-YFP* as well as in the double and triple transgenic lines reach only about 20-25% of the levels detected in the *ProPHYA:PHYA-YFP* line. In these lines expression of *ProCAB3:PHYA-YFP* was restricted to the mesophyll/subepidermal cells of the cotyledon and the hook region of the hypocotyl, whereas it was also highly expressed in other parts of the hypocotyl in the *ProPHYA:PHYA-YFP* lines. Nevertheless, phyA signaling restricted to these cells restored up to 50% of the FR-sensitized phototropic response in transgenic *phyA-201* mutants that expressed the *ProCAB3:PHYA-YFP* or *ProML1+ProCAB3+ProSUC2:PHYA-YFP* but not the *ProML1:PHYA-YFP* or *ProSUC2:PHYA-YFP* transgenes (Fig. 3). Thus we hypothesize that phyA presence in the subepidermal cells of hook is critical to regulate this response, and signaling by the photoreceptor from other tissues/cells might have limited importance. This hypothesis is in harmony with findings demonstrating that cellular re-distribution of PHOTOTROPIN1 is mediated by FR and takes place in the upper part of hypocotyls (Han *et al.*, 2008) and also with a more recent study investigating the spatial features of PHOTOTROPIN1-mediated blue light dependent phototropism (Preuten *et al.*, 2013). However, phyA signaling in the mesophyll cells was also shown to contribute to restoring FR-induced expansion of the cotyledons of the *phyA-201* mutant but not to the regulation of flowering time or root elongation (Fig. 2, Fig. 4).

Expression of the *ProML1:PHYA-YFP* transgene was sufficient to restore FR-HIR induced root elongation of the *phyA-201* mutant, similarly to *ProPHYA:PHYA-YFP* (Fig. 2). It was reported that local phyA signaling in the root is dismissible (Costigan *et al.*, 2011), and shoot-derived, phyA-controlled signal regulates elongation of roots in FR (Salisbury *et al.*, 2007). Our data show that the action of phyA in the mesophyll cells or vasculature is not required and phyA in the root of *ProML1:PHYA-YFP* line is expressed only in a few epidermis cells located at the boundary of dividing/elongation zone (Fig. S9,S10). Thus we conclude that the signal is likely generated by the action of phyA of epidermal location in the hypocotyls, cotyledons but not in the root (Fig. S9,S10) It is assumed that auxin plays a critical role in regulating root elongation. However, it remains to be determined how signaling by phyA in the epidermis modulates local synthesis and/or transport of auxin to promote root elongation

(Grieneisen *et al.*, 2007). *phyA* localized in the epidermis also contributes to inhibition of hypocotyl elongation and cotyledon expansion (Fig. 2), but not to the regulation of flowering time (Fig. 4) or phototropism (Fig. 3).

The triple transgenic lines, with the exception of the partially restored inhibition of hypocotyl elongation and phototropism, exhibited fully complemented *phyA-201* phenotype. Since *phyA-YFP* in the epidermis and vascular tissues are expressed approximately at the same level in these plants as in the *ProPHYA:PHYA-YFP* we conclude that the action of *phyA* in the mesophyll cells is critical for the regulation of hypocotyl elongation. This is in good agreement with recent findings obtained by analyzing this response in transgenic lines in which the chromophore was depleted in the mesophyll cells (Warnasooriya & Montgomery, 2009) or *phyB* was expressed in the mesophyll cells of the cotyledon (Endo *et al.*, 2005). These authors also concluded that the long-distance signal produced in the cotyledons is required for the regulation of hypocotyl growth inhibition. The transgenic lines used in this study are not suitable to study organ-specific signaling, yet we note that the triple transgenic lines had fully developed cotyledons and roots. The apparent contradiction between our data and those published by (Warnasooriya & Montgomery, 2009) can be explained by three mutually non-exclusive mechanisms. Namely, we assume that either (i) the signal derived from the mesophyll cells is insufficient to exclusively regulate hypocotyl growth because of the sub-optimally low level accumulation of *phyA* brought about by the *ProCAB3:PHYA-YFP* transgene (ii) in addition to the mesophyll cells, local *phyA* action in other cell types (epidermis) of the hypocotyl is also required, or (iii) despite the fully complemented size the “metabolic state” of cotyledons of the triple transgenic line is still different from that of the *ProPHYA:PHYA-YFP* plants, thus the amount of the unknown signaling compound is suboptimal.

We have compared at molecular level *phyA* signaling in the different tissues to understand how *phyA* signaling in different tissues is integrated to control complex developmental processes such as hypocotyl growth. The data obtained by analyzing the expression pattern and level of a number of custom-designed molecular reporter constructs in the transgenic plants convincingly demonstrated that *phyA* (i) regulates the abundance of key regulatory transcription factors in a tissue-autonomous fashion, but (ii) also alters the expression of genes in cells lacking the photoreceptor via intercellular, cell-to-cell signaling under the experimental conditions used. Light-driven inactivation of COP1 is a key early step in photoreceptor-controlled signaling.

611 It has been shown that FR light activated phyA disrupts the COP1/SPA signaling
 612 complex by interacting with SPA1, which modifies the substrate specificity/activity of
 613 COP1 and thereby promotes accumulation of HY5 (Sheerin *et al.*, 2015).
 614 Interestingly, the SPA1 protein expressed in tissue-specific fashion was shown,
 615 similarly to phyA, to regulate flowering time in tissue-autonomous fashion and to
 616 modulate leaf expansion and hypocotyl growth also via initiating cell-to-cell signaling
 617 (Ranjan *et al.*, 2011). These and our data indicate that (i) cFR light mediated
 618 inactivation of the COP1/SPA1 complex only occurs in cells which do contain phyA,
 619 and (ii) the signal mediating cell-to-cell communication is generated by the action of
 620 phyA/SPA1/COP1 complex via modulating the abundance/activity of HY5 or other
 621 downstream components. This hypothesis is evidently supported by Fig. 5
 622 demonstrating that FR treatment increases the amount of HY5-GFP fusion protein in
 623 tissue-autonomous fashion. Of the bHLH-type PIF1 was shown to interact in a
 624 conformation-dependent fashion with phyA (Khanna *et al.*, 2004) and to be
 625 subsequently phosphorylated and degraded by the 26S proteasome (Al-Sady *et al.*,
 626 2006; Shen *et al.*, 2008). Our data show that (i) FR induced degradation of the
 627 negative regulatory factor PIF1 (Fig. 6) occurs in a tissue-specific fashion, and (ii) this
 628 process does not generate transmittable, non-cell autonomous signal(s) that would
 629 facilitate the degradation of PIF1 in cells of neighboring tissues free of phyA-YFP.
 630 Recent reports provided a conceptual framework for the integration of phytochrome
 631 and phytohormone signaling (de Lucas *et al.*, 2008; Feng *et al.*, 2008; Franklin *et al.*,
 632 2011; Bai *et al.*, 2012; Oh *et al.*, 2012; Zhong *et al.*, 2012); however, these models
 633 need to be adapted to the cellular level to understand synchronization of elongation of
 634 individual cells in different tissues. The tissue/cell-autonomous regulation of key TFs
 635 and phyA association with the promoters of hundreds of genes (Chen *et al.*, 2014)
 636 explain the partially complemented phenotype of tissue-specifically expressed phyA-
 637 YFP and shows that ubiquitous expression of and simultaneous signaling by phyA in
 638 different cells is essential for the control of hypocotyl and cotyledon growth.
 639 However, our data also show altered transcription of *ProGA2ox1* and *ProXTH17* in
 640 cells lacking phyA. We assume that transcription of these genes is not mediated by
 641 HY5 and/or PIFs or phyA associated with the promoters of these genes, since the
 642 abundance of these TFs as well as the substrate specificity of the COP1/SPA complex
 643 do not change upon FR irradiation in those cells which do not contain phyA-YFP. FR
 644 down-regulated transcription of *ProIAA19* represents a yet different mode of phyA

action. It appears to require efficient phyA signaling in the mesophyll and epidermis or only in the mesophyll cells, since FR down-regulation of *ProIAA19* transcription is detectable only in WT but not in the *ProML1:PHYA-YFP* and triple transgenic line (Fig. 7). The relatively lower abundance of phyA-YFP in mesophyll cells supports this conclusion. *ProIAA19* transcription was shown to be regulated by coordinated action of HY5 and the PICKLE (chromatin remodeller) in the hypocotyl in cFR light (Jing *et al.*, 2013). Our data indicate that PICKLE-regulated action of HY5 is either not manifested in epidermis cells or requires a yet unknown factor. It is evident that transcriptional regulation of *ProGA2ox1*, *ProXTH17* and *ProIAA19* is mediated by intercellular signaling dependent on phyA action. At present we do not have data at the whole genome level to estimate the number of genes whose expression is controlled by intercellular signaling dependent on phyA action, nor about the chemical nature of these signals. As far the biological function of phyA-controlled intercellular signaling is concerned, we speculate that it likely provides an additional regulatory layer to fine-tune integration of signaling cascades induced by light and other biotic and abiotic factors.

ACKNOWLEDGEMENT

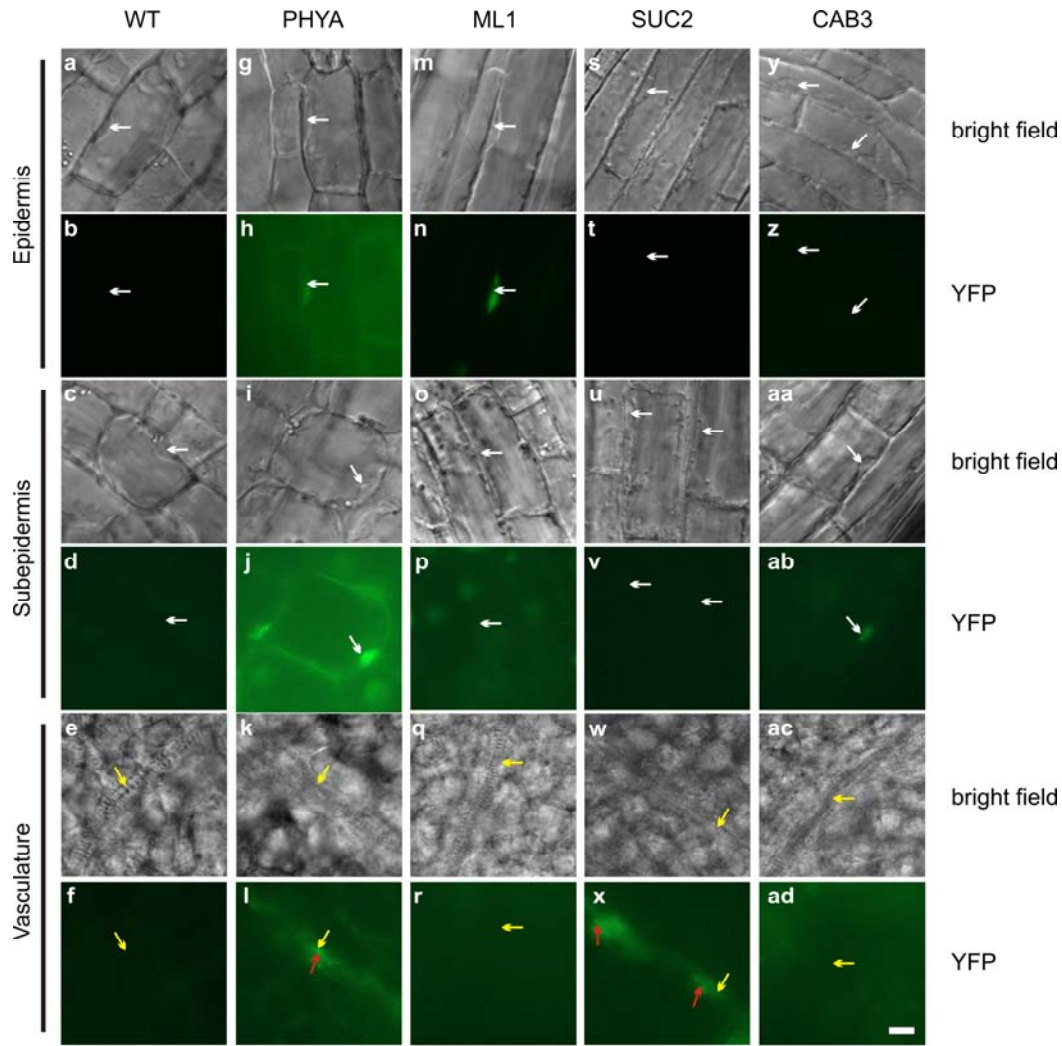
We thank Ferhan Ayaydin for the help with the confocal laser scanning microscope. Work in Freiburg, was supported by DFG grants to E.S., S.K. (SFB 592, KI 1077/2) and A. H. (HI 1369/5-1), an HFSP grant to A.H. (RGP0025/2013) and the Excellence Initiative of the German Federal and State Governments (EXC 294) to A.H.. Work in Hungary was supported by Hungarian Scientific Research Fund (OTKA, K-108559 and NN-110636) and TAMOP-4.2.2.A-11/1/KONV-2012-0035 grants to F.N. and a János Bolyai Research Scholarship to A.V., whereas work in Edinburgh was supported by BBSRC grant BB/K006975/1 to F.N.

AUTHOR CONTRIBUTION

D.K., A.V., S.K., E.A., M.L., A.H., C.K., Z.H. performed research; E.S. and F.N. designed the research and analyzed data; F.N. wrote the paper.

679 **FIGURES AND FIGURE LEGENDS**

680



Kirchenbauer et al., Figure 1

681

682 **Figure 1**

683 **phyA-YFP is localized exclusively in the epidermal or mesophyll or vascular cells**

684 **of the selected transgenic Arabidopsis *phyA-201* seedlings.** Localization of the

685 fusion protein was monitored by epifluorescence microscopy in the hook region [a-d,

686 g-j, m-p, s-v, y-ab] and cotyledons [e, f, k, l, q, r, w, x, ac, ad] of seedlings grown

687 for 2 days in cFR light ($20 \mu\text{mol m}^{-2} \text{sec}^{-1}$). To facilitate comparison of the expression

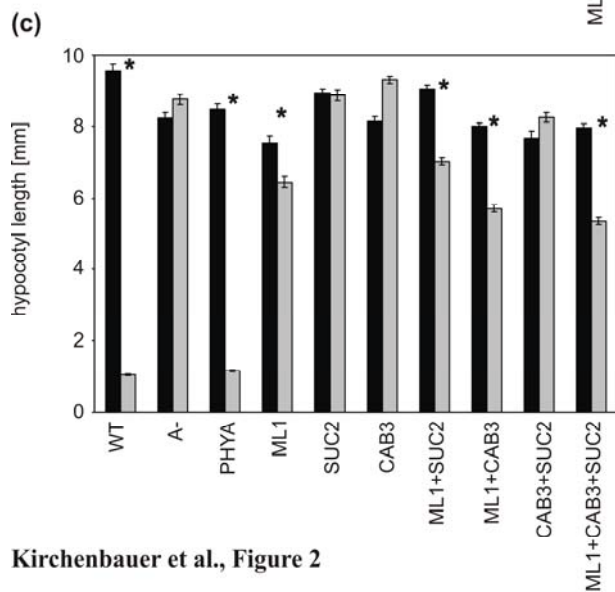
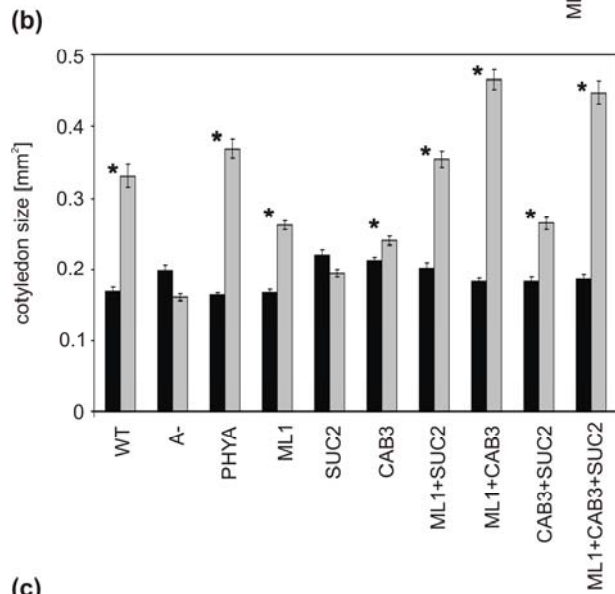
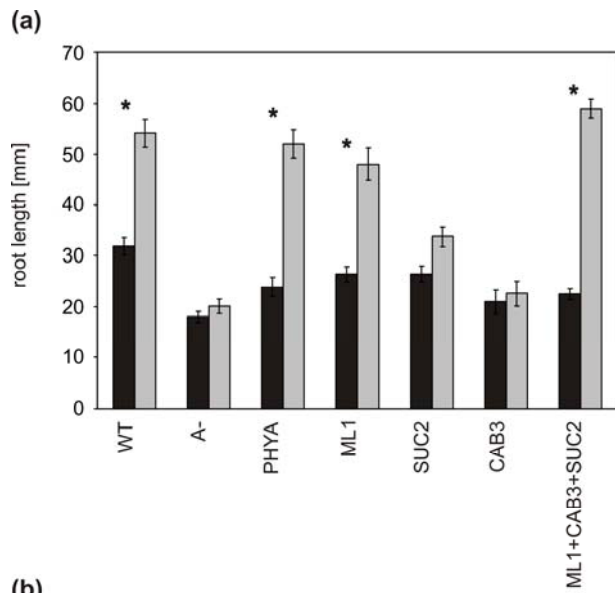
688 level of phyA-YFP in the tissues of the lines, all images showing the same tissue were

689 obtained after identical exposure times. phyA-YFP is expressed ubiquitously in the

690 *ProPHYA:PHYA-YFP* seedlings [g, i, k bright field microscopy; h, j, l

691 epifluorescence microscopy], it is expressed only in the epidermal cells in the

692 *ProML1:PHYA-YFP* lines [**m, o, q** bright field microscopy; **n, p, r** epifluorescence
693 microscopy], it shows vascular specific expression in the *ProSUC2:PHYA-YFP* plants
694 [**s, u, v** bright field microscopy; **t, v, x** epifluorescent microscopy] and is exclusively
695 localized in the sub-epidermal, mesophyll cells in the *ProCAB3:PHYA-YFP* seedlings
696 [**y, aa, ac** bright field microscopy; **z, ab, ad** epifluorescence microscopy]. White
697 arrows mark positions of selected nuclei, yellow arrows point at vascular bundles, red
698 arrows indicate vascular YFP signal. Scale bar = 10 μ m. Legend: WT = Ler
699 (Landsberg *erecta*); PHYA = *ProPHYA:PHYA-YFP*; ML1 = *ProML1:PHYA-YFP*;
700 SUC2 = *ProSUC2:PHYA-YFP*; CAB3 = *ProCAB3:PHYA-YFP*. Each transgene is
701 expressed in *phyA-201* background.
702



Kirchenbauer et al., Figure 2

704 **Figure 2**

705 **Phenotypic analyses of Arabidopsis seedlings expressing phyA-YFP in different**

706 **tissues.**

707 **(a) phyA-YFP expressed in the epidermis can restore FR-promoted root**

708 **elongation in the *phyA-201* mutant**

709 Seedlings were grown on vertically positioned ½ MS plates for 10 days in dark or

710 under continuous FR irradiation and their root length was measured. For detailed

711 legend see the legend of Figure 2C.

712 **(b) Tissue-specifically expressed phyA-YFP promotes cotyledon expansion of the**

713 ***phyA-201* mutant in FR light.** After induction of germination transgenic seedlings

714 were grown for 3 days in constant dark or illuminated with FR light ($20 \mu\text{mol m}^{-2} \text{s}^{-1}$).

715 Absolute surface area of cotyledons (mm^2) is shown [black columns (dark) and gray

716 columns (far-red)]. For detailed legend see the legend of Figure 2C.

717 **(c) phyA-YFP localized in the epidermis partially restores FR light promoted**

718 **inhibition of hypocotyl elongation of the *phyA-201* mutant.** After induction of

719 germination, transgenic seedlings were grown for 3 days in constant dark or

720 illuminated with FR light ($20 \mu\text{mol m}^{-2} \text{s}^{-1}$). Absolute hypocotyl lengths (mm) are

721 shown [black columns (dark) and gray columns (far-red)]. Legend: WT = Ler ; A- =

722 *phyA-201*; PHYA = *ProPHYA:PHYA-YFP*; ML1 = *ProML1:PHYA-YFP*; SUC2 =

723 *ProSUC2:PHYA-YFP*; CAB3 = *ProCAB3:PHYA-YFP*; ML1+SUC2 =

724 *ProML1:PHYA-YFP* x *ProSUC2:PHYA-YFP*; ML1+CAB3= *ProML1:PHYA-YFP* x

725 *ProCAB3:PHYA-YFP*; CAB3+SUC2 = *ProCAB3:PHYA-YFP* x *ProSUC2:PHYA-*

726 *YFP*; ML1+CAB3+SUC2= *ProML1:PHYA-YFP* x *ProCAB3:PHYA-YFP* x

727 *ProSUC2:PHYA-YFP*. Each transgene is expressed in *phyA-201* background. Bars

728 indicate mean of at least 25 seedlings, error bars represent standard error, asterisks

729 mark lines that display significant differences by the Mann-Whitney U test

730 (significance $P < 0.01$) after far-red treatment.

731

732

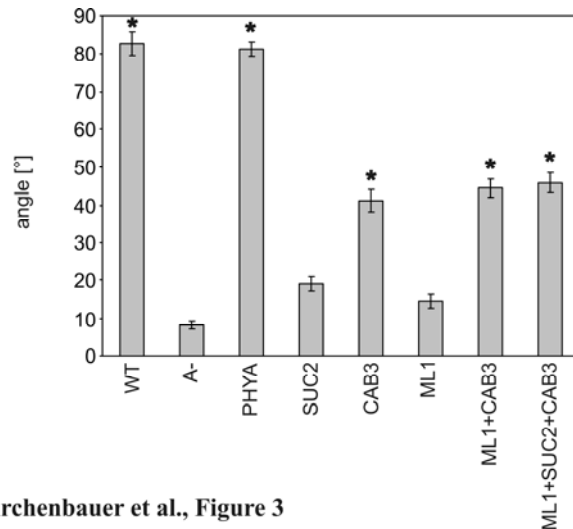
733

734

735

736

737

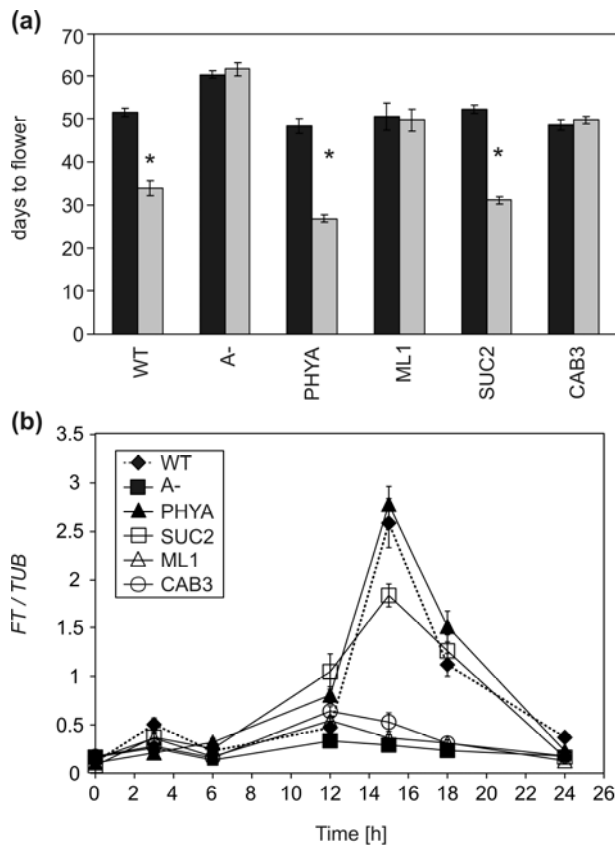


Kirchenbauer et al., Figure 3

Figure 3

phyA-YFP expressed in mesophyll cells efficiently promotes phototropism in blue light

Arabidopsis seedlings were grown in darkness for 2 days on vertical ½ MS plates and were irradiated first with far-red light ($10 \mu\text{mol m}^{-2} \text{s}^{-1}$) for 120 min and subsequently exposed to unilateral blue light ($1 \mu\text{mol m}^{-2} \text{s}^{-1}$) for 160 min. The angle of hypocotyl bending is shown, error bars represent standard error, asterisks indicate significant response by the Mann-Whitney U test ($P < 0.01$) compared to the *phyA-201* mutant. For the detailed name of examined lines see the legend of Figure 2C.



Kirchenbauer et al., Figure 4

Figure 4

phyA-YFP localized in vascular tissue complements flowering phenotype of the *Arabidopsis phyA-201* mutant and elevates *FT* mRNA levels

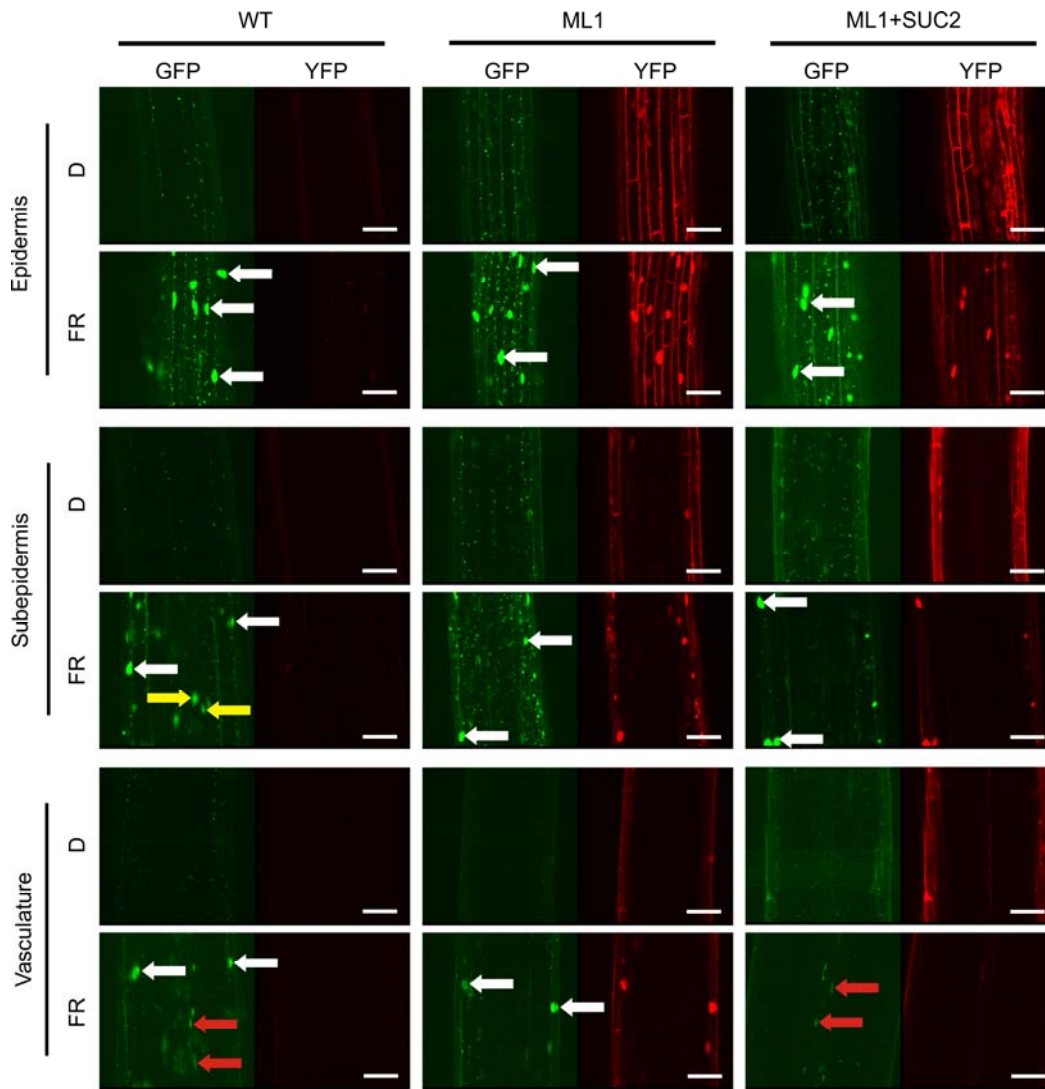
(a) Analysis of the flowering time.

Examined seedlings were grown in short day with (gray bars) or without (black bars) 8 h FR light ($30 \mu\text{mol m}^{-2} \text{s}^{-1}$) day extension for 15 days. After day 15 all plants were grown in short day without FR irradiation. Bars indicate the number of days to bolting. The experiment was repeated 3 times, error bars show standard error of the mean; asterisks indicate significant response by the Mann-Whitney U test ($P < 0.01$) compared to the *phyA-201* mutant. For the detailed name of examined lines see the legend of Figure 2C.

(b) Effect of PHYA-YFP on *FT* transcript level

Transgenic seedlings were grown in short day with FR light day extension as described above. On day 14 samples were collected at the indicated time points and total RNA was isolated. Expression level of *FT* was analyzed by qRT-PCR and the obtained values were normalized to the corresponding *TUBULIN (TUB)* mRNA

779 amount. Error bars indicate the standard error of the mean values obtained from three
780 independent experiments. For the detailed name of examined lines see the legend of
781 Figure 2C.



Kirchenbauer et al., Figure 5

783

784

Figure 5

785

phyA-YFP controls FR-induced accumulation of HY5-GFP in tissue-autonomous fashion.

786

787

Arabidopsis Ler (WT), and *phyA-201* mutant seedlings harboring *ProML1:PHYA-*

788

YFP (ML1) or *ProML1+ProSUC2:PHYA-YFP* (ML1+SUC2) transgene expressing

789

the *ProHY5:HY5-GFP* reporter were grown in darkness (D) for 4 days and irradiated

790

with $10 \mu\text{mol m}^{-2} \text{s}^{-1}$ 4 h FR light (FR). Localization and abundance of HY5-GFP

791

(GFP) and PHYA-YFP (YFP) were monitored by confocal laser scanning

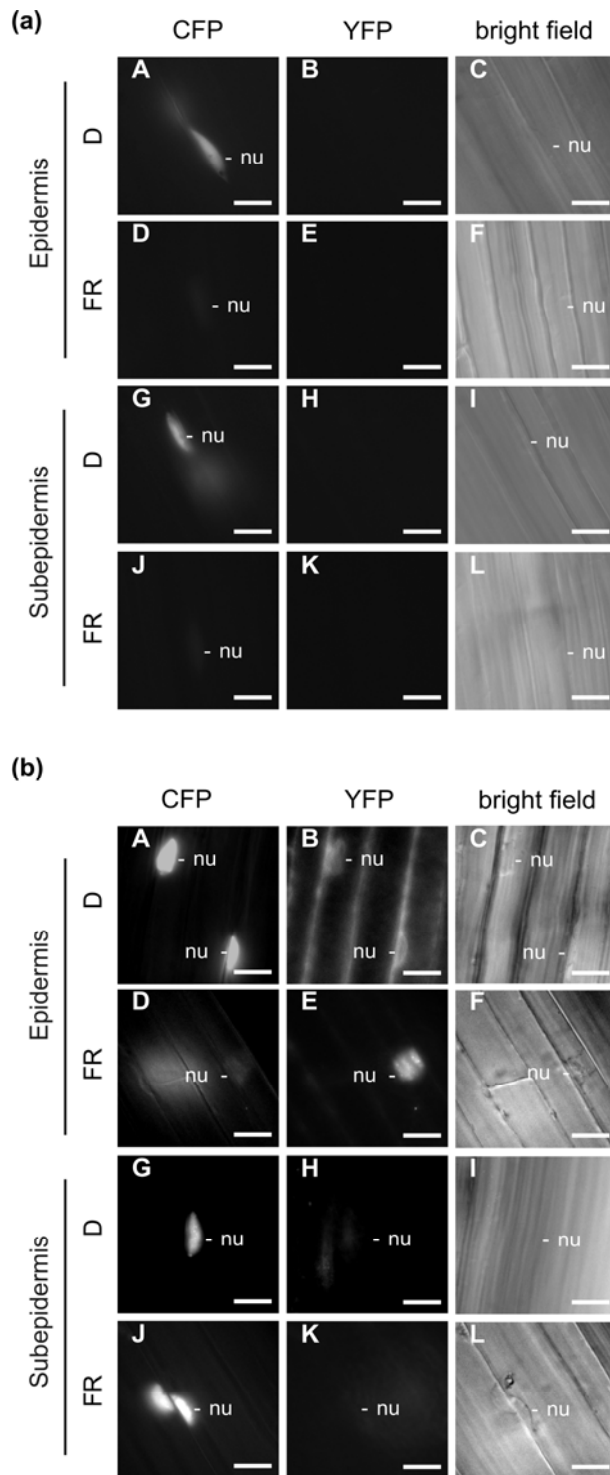
792

microscopy. To facilitate comparison of the expression levels of HY5-GFP in

793

different tissues, all images shown were obtained after identical exposure settings.

794 White arrows mark nuclei in the epidermis, yellow arrows point to nuclei in the sub-
795 epidermal layer, whereas red arrows indicate nuclei in the vasculature. Scale bar = 50
796 μm .
797
798



Kirchenbauer et al., Figure 6

Figure 6

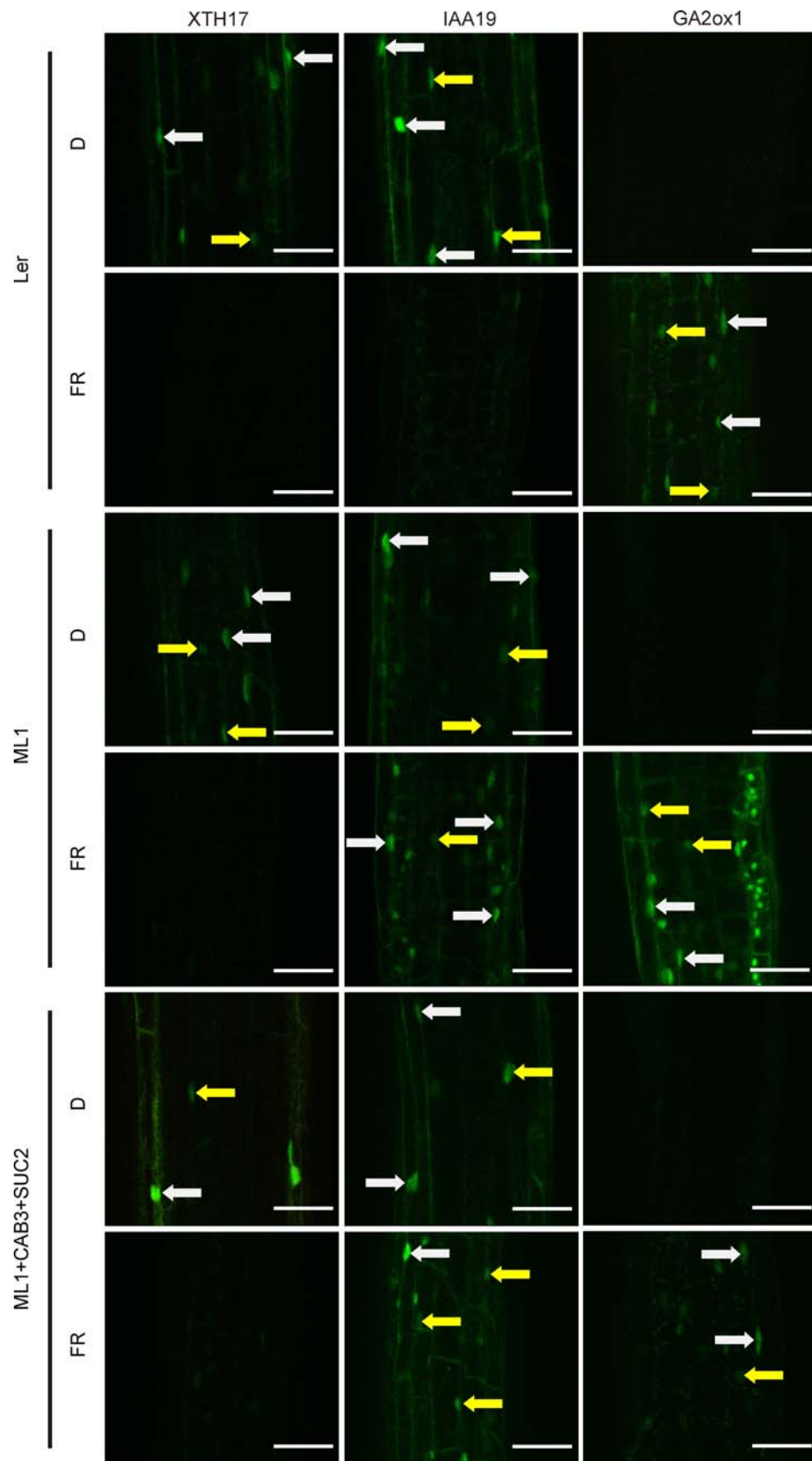
phyA controls FR induced degradation of CFP-PIF1 fusion protein in tissue-autonomous fashion.

803 **(a) CFP-PIF1 degradation in Arabidopsis Ler wild-type seedlings.** WT seedlings
804 expressing the *Pro35S:CFP-PIF1* transgene were grown in darkness for 4 days and
805 either irradiated with FR light ($20 \mu\text{mol m}^{-2} \text{s}^{-1}$) for 24 h (**D, E, F, J, K, L**) or further
806 kept in darkness (**A, B, C, G, H, I**). Localization and abundance of the CFP-PIF1
807 fusion protein were monitored by epifluorescence microscopy on the 5th day with
808 specific filter sets in the epidermis (**A-F**) or subepidermal cell layer (**G-L**) and
809 representative cells are shown. Positions of nuclei pair-wise analyzed for CFP
810 fluorescence (**A, D, G, J**) or YFP (**B, E, H, K**) are marked by nu. **C, F, I, L** show the
811 respective transmitted light images.

812 **(b) CFP-PIF1 degradation in transgenic Arabidopsis *phyA-201* seedlings**
813 **expressing *ProML1:PHYA-YFP*.** Localization and abundance of the phyA-YFP and
814 CFP- PIF1 fusion proteins were monitored by epifluorescence microscopy in
815 transgenic *ProML1:PHYA-YFP* seedlings expressing the *Pro35S:CFP-PIF1* treated as
816 described above.

817 Note that (**A, B, C**) and (**G, H, I**) as well as (**D, E, F**) and (**J, K, L**) in Figure 6A and
818 Figure 6B represent the epidermal or subepidermal plane, respectively, at the same
819 location within the hypocotyl. Scale bar = 10 μm .

820
821



Kirchenbauer et al., Figure 7

Figure 7

Different spatial patterns of FR-controlled *ProXTH1*, *ProIAA19* and *ProGA2ox1* promoter activity in hypocotyl cells

Arabidopsis Ler (WT), and *phyA-201* mutant seedlings harboring *ProML1:PHYA-YFP* (ML1) or *ProML1+ProCAB3+ProSUC2:PHYA-YFP* (ML1+CBA3+SUC2) transgenes expressing *ProXTH17:CFP-NLS* or *ProIAA19:CFP-NLS* or *ProGA2ox1:CFP-NLS* reporters were grown in darkness for 4 days (D) and subsequently irradiated with 16 h FR light ($10 \mu\text{mol m}^{-2} \text{s}^{-1}$) (FR). Localization and abundance of the CFP-NLS fluorophore was monitored in the hypocotyl tissues by confocal laser scanning microscopy. White arrows mark nuclei in the epidermis, yellow arrows point to nuclei in the sub-epidermal layer. Scale bar = 50 μm .

REFERENCES

- Adam E, Kircher S, Liu P, Merai Z, Gonzalez-Schain N, Horner M, Viczian A, Monte E, Sharrock RA, Schafer E, et al. 2013. Comparative functional analysis of full-length and N-terminal fragments of phytochrome C, D and E in red light-induced signaling. *New Phytol* **200**(1): 86-96.
- Al-Sady B, Ni W, Kircher S, Schafer E, Quail PH. 2006. Photoactivated phytochrome induces rapid PIF3 phosphorylation prior to proteasome-mediated degradation. *Mol Cell* **23**(3): 439-446.
- Bai MY, Shang JX, Oh E, Fan M, Bai Y, Zentella R, Sun TP, Wang ZY. 2012. Brassinosteroid, gibberellin and phytochrome impinge on a common transcription module in Arabidopsis. *Nat Cell Biol* **14**(8): 810-817.
- Bauer D, Viczian A, Kircher S, Nobis T, Nitschke R, Kunkel T, Panigrahi KC, Adam E, Fejes E, Schafer E, et al. 2004. Constitutive photomorphogenesis 1 and multiple photoreceptors control degradation of phytochrome interacting factor 3, a transcription factor required for light signaling in Arabidopsis. *Plant Cell* **16**(6): 1433-1445.
- Bischoff F, Millar AJ, Kay SA, Furuya M. 1997. Phytochrome-induced intercellular signalling activates *cab::luciferase* gene expression. *The Plant Journal* **12**(4): 839-849.

856 **Bowler C, Neuhaus G, Yamagata H, Chua NH. 1994.** Cyclic GMP and calcium
857 mediate phytochrome phototransduction. *Cell* **77**(1): 73-81.

858 **Casal JJ, Candia AN, Sellaro R. 2014.** Light perception and signalling by
859 phytochrome A. *J Exp Bot* **65**(11): 2835-2845.

860 **Casal JJ, Smith H. 1988a.** The loci of perception for phytochrome control of
861 internode growth in light-grown mustard: Promotion by low phytochrome
862 photoequilibria in the internode is enhanced by blue light perceived by the leaves.
863 *Planta* **176**(2): 277-282.

864 **Casal JJ, Smith H. 1988b.** Persistent effects of changes in phytochrome status on
865 internode growth in light-grown mustard: Occurrence, kinetics and locus of
866 perception. *Planta* **175**(2): 214-220.

867 **Chaves I, Pokorny R, Byrdin M, Hoang N, Ritz T, Brettel K, Essen LO, van der**
868 **Horst GT, Batschauer A, Ahmad M. 2011.** The cryptochromes: blue light
869 photoreceptors in plants and animals. *Annu Rev Plant Biol* **62**: 335-364.

870 **Chen F, Li B, Li G, Charron JB, Dai M, Shi X, Deng XW. 2014.** Arabidopsis
871 Phytochrome A Directly Targets Numerous Promoters for Individualized Modulation
872 of Genes in a Wide Range of Pathways. *Plant Cell* **26**(5): 1949-1966.

873 **Christie JM. 2007.** Phototropin blue-light receptors. *Annu Rev Plant Biol* **58**: 21-45.

874 **Clack T, Mathews S, Sharrock RA. 1994.** The phytochrome apoprotein family in
875 Arabidopsis is encoded by five genes: the sequences and expression of *PHYD* and
876 *PHYE*. *Plant Mol Biol* **25**(3): 413-427.

877 **Clough SJ, Bent AF. 1998.** Floral dip: a simplified method for Agrobacterium-
878 mediated transformation of *Arabidopsis thaliana*. *Plant J* **16**(6): 735-743.

879 **Costigan SE, Warnasooriya SN, Humphries BA, Montgomery BL. 2011.** Root-
880 localized phytochrome chromophore synthesis is required for photoregulation of root
881 elongation and impacts root sensitivity to jasmonic acid in Arabidopsis. *Plant Physiol*
882 **157**(3): 1138-1150.

883 **de Lucas M, Daviere JM, Rodriguez-Falcon M, Pontin M, Iglesias-Pedraz JM,**
884 **Lorrain S, Fankhauser C, Blazquez MA, Titarenko E, Prat S. 2008.** A molecular
885 framework for light and gibberellin control of cell elongation. *Nature* **451**(7177): 480-
886 484.

887 **Endo M, Mochizuki N, Suzuki T, Nagatani A. 2007.** CRYPTOCHROME2 in
888 vascular bundles regulates flowering in Arabidopsis. *Plant Cell* **19**(1): 84-93.

889 **Endo M, Nakamura S, Araki T, Mochizuki N, Nagatani A. 2005.** Phytochrome B
890 in the mesophyll delays flowering by suppressing FLOWERING LOCUS T
891 expression in Arabidopsis vascular bundles. *Plant Cell* **17**(7): 1941-1952.

892 **Endo M, Tanigawa Y, Murakami T, Araki T, Nagatani A. 2013.**
893 *PHYTOCHROME-DEPENDENT LATE-FLOWERING* accelerates flowering through
894 physical interactions with phytochrome B and CONSTANS. *Proc Natl Acad Sci U S*
895 *A* **110**(44): 18017-18022.

896 **Feng S, Martinez C, Gusmaroli G, Wang Y, Zhou J, Wang F, Chen L, Yu L,**
897 **Iglesias-Pedraz JM, Kircher S, et al. 2008.** Coordinated regulation of *Arabidopsis*
898 *thaliana* development by light and gibberellins. *Nature* **451**(7177): 475-479.

899 **Franklin KA, Lee SH, Patel D, Kumar SV, Spartz AK, Gu C, Ye S, Yu P, Breen**
900 **G, Cohen JD, et al. 2011.** Phytochrome-interacting factor 4 (PIF4) regulates auxin
901 biosynthesis at high temperature. *Proc Natl Acad Sci U S A* **108**(50): 20231-20235.

902 **Franklin KA, Quail PH. 2010.** Phytochrome functions in Arabidopsis development.
903 *J Exp Bot* **61**(1): 11-24.

904 **Grieneisen VA, Xu J, Maree AF, Hogeweg P, Scheres B. 2007.** Auxin transport is
905 sufficient to generate a maximum and gradient guiding root growth. *Nature*
906 **449**(7165): 1008-1013.

907 **Hall A, Kozma-Bognar L, Toth R, Nagy F, Millar AJ. 2001.** Conditional circadian
908 regulation of *PHYTOCHROME A* gene expression. *Plant Physiol* **127**(4): 1808-1818.

909 **Han IS, Tseng TS, Eisinger W, Briggs WR. 2008.** Phytochrome A regulates the
910 intracellular distribution of phototropin 1-green fluorescent protein in *Arabidopsis*
911 *thaliana*. *Plant Cell* **20**(10): 2835-2847.

912 **Hategan L, Godza B, Kozma-Bognar L, Bishop GJ, Szekeres M. 2014.**
913 Differential expression of the brassinosteroid receptor-encoding *BRI1* gene in
914 Arabidopsis. *Planta* **239**(5): 989-1001.

915 **Hiltbrunner A, Tscheuschler A, Viczian A, Kunkel T, Kircher S, Schafer E.**
916 **2006.** *FHY1* and *FHL* act together to mediate nuclear accumulation of the
917 phytochrome A photoreceptor. *Plant Cell Physiol* **47**(8): 1023-1034.

918 **Hiltbrunner A, Viczian A, Bury E, Tscheuschler A, Kircher S, Toth R,**
919 **Honsberger A, Nagy F, Fankhauser C, Schafer E. 2005.** Nuclear accumulation of
920 the phytochrome A photoreceptor requires *FHY1*. *Curr Biol* **15**(23): 2125-2130.

921 **Huq E, Al-Sady B, Hudson M, Kim C, Apel K, Quail PH. 2004.** Phytochrome-
 922 interacting factor 1 is a critical bHLH regulator of chlorophyll biosynthesis. *Science*
 923 **305**(5692): 1937-1941.

924 **Janoudi AK, Gordon WR, Wagner D, Quail P, Poff KL. 1997.** Multiple
 925 phytochromes are involved in red-light-induced enhancement of first-positive
 926 phototropism in *Arabidopsis thaliana*. *Plant Physiol* **113**(3): 975-979.

927 **Jing Y, Zhang D, Wang X, Tang W, Wang W, Huai J, Xu G, Chen D, Li Y, Lin**
 928 **R. 2013.** *Arabidopsis* chromatin remodeling factor PICKLE interacts with
 929 transcription factor HY5 to regulate hypocotyl cell elongation. *Plant Cell* **25**(1): 242-
 930 256.

931 **Johnson E, Bradley M, Harberd NP, Whitelam GC. 1994.** Photoresponses of
 932 Light-Grown phyA Mutants of *Arabidopsis* (Phytochrome A Is Required for the
 933 Perception of Daylength Extensions). *Plant Physiol* **105**(1): 141-149.

934 **Kami C, Hersch M, Trevisan M, Genoud T, Hiltbrunner A, Bergmann S,**
 935 **Fankhauser C. 2012.** Nuclear phytochrome A signaling promotes phototropism in
 936 *Arabidopsis*. *Plant Cell* **24**(2): 566-576.

937 **Khanna R, Huq E, Kikis EA, Al-Sady B, Lanzatella C, Quail PH. 2004.** A novel
 938 molecular recognition motif necessary for targeting photoactivated phytochrome
 939 signaling to specific basic helix-loop-helix transcription factors. *Plant Cell* **16**(11):
 940 3033-3044.

941 **Kircher S, Kozma-Bognar L, Kim L, Adam E, Harter K, Schafer E, Nagy F.**
 942 **1999.** Light quality-dependent nuclear import of the plant photoreceptors
 943 phytochrome A and B. *Plant Cell* **11**(8): 1445-1456.

944 **Kunkel T, Neuhaus G, Batschauer A, Chua NH, Schafer E. 1996.** Functional
 945 analysis of yeast-derived phytochrome A and B phycocyanobilin adducts. *Plant J*
 946 **10**(4): 625-636.

947 **Leivar P, Monte E, Cohn MM, Quail PH. 2012.** Phytochrome Signaling in Green
 948 *Arabidopsis* Seedlings: Impact Assessment of a Mutually Negative phyB–PIF
 949 Feedback Loop. *Molecular Plant* **5**(3): 734-749.

950 **Liscum E, Reed JW. 2002.** Genetics of Aux/IAA and ARF action in plant growth
 951 and development. *Plant Mol Biol* **49**(3-4): 387-400.

952 **Ma L, Li J, Qu L, Hager J, Chen Z, Zhao H, Deng XW. 2001.** Light control of
 953 *Arabidopsis* development entails coordinated regulation of genome expression and
 954 cellular pathways. *Plant Cell* **13**(12): 2589-2607.

955 **Mockler T, Yang H, Yu X, Parikh D, Cheng YC, Dolan S, Lin C. 2003.**
 956 Regulation of photoperiodic flowering by Arabidopsis photoreceptors. *Proc Natl*
 957 *Acad Sci U S A* **100**(4): 2140-2145.
 958 **Neff MM, Chory J. 1998.** Genetic interactions between phytochrome A,
 959 phytochrome B, and cryptochrome 1 during Arabidopsis development. *Plant Physiol*
 960 **118**(1): 27-35.
 961 **Neuhaus G, Bowler C, Kern R, Chua NH. 1993.** Calcium/calmodulin-dependent
 962 and -independent phytochrome signal transduction pathways. *Cell* **73**(5): 937-952.
 963 **Nick P, Ehmann B, Furuya M, Schafer E. 1993.** Cell Communication, Stochastic
 964 Cell Responses, and Anthocyanin Pattern in Mustard Cotyledons. *Plant Cell* **5**(5):
 965 541-552.
 966 **Oh E, Zhu JY, Wang ZY. 2012.** Interaction between BZR1 and PIF4 integrates
 967 brassinosteroid and environmental responses. *Nat Cell Biol* **14**(8): 802-809.
 968 **Osterlund MT, Hardtke CS, Wei N, Deng XW. 2000.** Targeted destabilization of
 969 HY5 during light-regulated development of Arabidopsis. *Nature* **405**(6785): 462-466.
 970 **Peschke F, Kretsch T. 2011.** Genome-wide analysis of light-dependent transcript
 971 accumulation patterns during early stages of Arabidopsis seedling deetiolation. *Plant*
 972 *Physiol* **155**(3): 1353-1366.
 973 **Preuten T, Hohm T, Bergmann S, Fankhauser C. 2013.** Defining the site of light
 974 perception and initiation of phototropism in Arabidopsis. *Curr Biol* **23**(19): 1934-
 975 1938.
 976 **Ranjan A, Fiene G, Fackendahl P, Hoecker U. 2011.** The Arabidopsis repressor of
 977 light signaling *SPA1* acts in the phloem to regulate seedling de-etiolation, leaf
 978 expansion and flowering time. *Development* **138**(9): 1851-1862.
 979 **Rausenberger J, Tscheuschler A, Nordmeier W, Wust F, Timmer J, Schafer E,**
 980 **Fleck C, Hiltbrunner A. 2011.** Photoconversion and nuclear trafficking cycles
 981 determine phytochrome A's response profile to far-red light. *Cell* **146**(5): 813-825.
 982 **Reed JW, Nagpal P, Poole DS, Furuya M, Chory J. 1993.** Mutations in the gene
 983 for the red/far-red light receptor phytochrome B alter cell elongation and
 984 physiological responses throughout Arabidopsis development. *Plant Cell* **5**(2): 147-
 985 157.
 986 **Rieu I, Eriksson S, Powers SJ, Gong F, Griffiths J, Woolley L, Benlloch R,**
 987 **Nilsson O, Thomas SG, Hedden P, et al. 2008.** Genetic analysis reveals that C19-

GA 2-oxidation is a major gibberellin inactivation pathway in Arabidopsis. *Plant Cell* **20**(9): 2420-2436.

Rizzini L, Favory JJ, Cloix C, Faggionato D, O'Hara A, Kaiserli E, Baumeister R, Schafer E, Nagy F, Jenkins GI, et al. 2011. Perception of UV-B by the Arabidopsis UVR8 protein. *Science* **332**(6025): 103-106.

Salisbury FJ, Hall A, Grierson CS, Halliday KJ. 2007. Phytochrome coordinates Arabidopsis shoot and root development. *Plant J* **50**(3): 429-438.

Sessions A, Weigel D, Yanofsky MF. 1999. The Arabidopsis thaliana *MERISTEM LAYER 1* promoter specifies epidermal expression in meristems and young primordia. *Plant J* **20**(2): 259-263.

Sharrock RA, Quail PH. 1989. Novel phytochrome sequences in Arabidopsis thaliana: structure, evolution, and differential expression of a plant regulatory photoreceptor family. *Genes Dev* **3**(11): 1745-1757.

Sheerin DJ, Menon C, zur Oven-Krockhaus S, Enderle B, Zhu L, Johnen P, Schleifenbaum F, Stierhof YD, Huq E, Hiltbrunner A. 2015. Light-activated phytochrome A and B interact with members of the SPA family to promote photomorphogenesis in Arabidopsis by reorganizing the COP1/SPA complex. *Plant Cell* **27**(1): 189-201.

Schneider C.A., Rasband W.S., Eliceiri K.W. (2012). NIH Image to ImageJ: 25 years of image analysis. *Nat Methods* **9**(7): 671-675.

Shen H, Zhu L, Castillon A, Majee M, Downie B, Huq E. 2008. Light-induced phosphorylation and degradation of the negative regulator PHYTOCHROME-INTERACTING FACTOR1 from Arabidopsis depend upon its direct physical interactions with photoactivated phytochromes. *Plant Cell* **20**(6): 1586-1602.

Somers DE, Quail PH. 1995. Temporal and spatial expression patterns of *PHYA* and *PHYB* genes in Arabidopsis. *Plant J* **7**(3): 413-427.

Srivastava AC, Ganesan S, Ismail IO, Ayre BG. 2008. Functional characterization of the Arabidopsis *AtSUC2* *Sucrose/H⁺ symporter* by tissue-specific complementation reveals an essential role in phloem loading but not in long-distance transport. *Plant Physiol* **148**(1): 200-211.

Tepperman JM, Zhu T, Chang HS, Wang X, Quail PH. 2001. Multiple transcription-factor genes are early targets of phytochrome A signaling. *Proc Natl Acad Sci U S A* **98**(16): 9437-9442.

1021 **Tian CE, Muto H, Higuchi K, Matamura T, Tatematsu K, Koshiba T,**
 1022 **Yamamoto KT. 2004.** Disruption and overexpression of *auxin response factor 8* gene
 1023 of Arabidopsis affect hypocotyl elongation and root growth habit, indicating its
 1024 possible involvement in auxin homeostasis in light condition. *Plant J* **40**(3): 333-343.
 1025 **Vissenberg K, Oyama M, Osato Y, Yokoyama R, Verbelen J-P, Nishitani K.**
 1026 **2005.** Differential Expression of *AtXTH17*, *AtXTH18*, *AtXTH19* and *AtXTH20* Genes
 1027 in Arabidopsis Roots. Physiological Roles in Specification in Cell Wall Construction.
 1028 *Plant and Cell Physiology* **46**(1): 192-200.
 1029 **Warnasooriya SN, Montgomery BL. 2009.** Detection of spatial-specific
 1030 phytochrome responses using targeted expression of biliverdin reductase in
 1031 Arabidopsis. *Plant Physiol* **149**(1): 424-433.
 1032 **Yu X, Liu H, Klejnot J, Lin C. 2010.** The Cryptochrome Blue Light Receptors.
 1033 *Arabidopsis Book* **8**: e0135.
 1034 **Zhong S, Shi H, Xue C, Wang L, Xi Y, Li J, Quail PH, Deng XW, Guo H. 2012.**
 1035 A molecular framework of light-controlled phytohormone action in Arabidopsis. *Curr*
 1036 *Biol* **22**(16): 1530-1535.

1041 **SUPPORTING INFORMATION**

1042 The following materials are available in the online version of this article.

1043 **Supporting Information Figures**

1044 Fig. S1

1045 Application of qRT-PCR method for the selection of homozygous transgenic
 1046 seedlings.

1047 Fig. S2

1048 Expression level of phyA-YFP in the selected transgenic lines.

1049 Fig. S3

1050 Determination of phyA-YFP accumulation at tissue level.

1051 Fig. S4

1052 Detection of PHYA-YFP in the epidermal and mesophyll tissues of the cotyledon.

1053 Fig. S5

1054 Detection of PHYA-YFP in the mesophyll and companion cells of the cotyledon.

1055 Fig. S6
1056 Detection of PHYA-YFP in the hook region of the hypocotyl.
1057 Fig. S7
1058 Detection of PHYA-YFP in the upper part of the hypocotyl.
1059 Fig. S8
1060 Detection of PHYA-YFP in the lower part of the hypocotyl.
1061 Fig. S9
1062 Detection of PHYA-YFP in the root.
1063 Fig. S10
1064 Detection of PHYA-YFP in the root tip.
1065 Fig. S11
1066 Root elongation, cotyledon expansion and inhibition of hypocotyl elongation
1067 regulated by phyA-YFP expressed in different tissues.
1068 Fig. S12
1069 phyA degradation in red light.
1070 Fig. S13
1071 phyA-YFP controls FR-induced accumulation of HY5-GFP in all tissue types
1072 examined.
1073 Fig. S14
1074 FR-regulated *ProXTH17* and *ProGA2ox1* promoter activity in cotyledon cells.
1075 **Supporting Information Tables**
1076 Table S1
1077 Sequences of oligonucleotides used in the study
1078 Table S2
1079 phyA-YFP detectability in different tissues
1080
1081 **Methods S1**
1082